DEUTSCHES ELEKTRONEN-SYNCHROTRON DESY

DESY SR-71/3
May 1971

Dielectric Properties of the Rubidium Halide Crystals in the Extreme Ultraviolet up to 30 eV

by

C. J. Peimann and M. Skibowski

2 HAMBURG 52 · NOTKESTIEG 1

To be sure that your preprints are promptly included in the HIGH ENERGY PHYSICS INDEX, send them to the following address (if possible by air mail):

DESY
Bibliothek
2 Hamburg 52
Notkestieg 1
Germany

Dielectric Properties of the Rubidium Halide Crystals in the Extreme Ultraviolet up to 30 eV

C.J. Peimann[+] and M. Skibowski[‡]

Deutsches Elektronen-Synchrotron DESY, Hamburg, Germany

The reflectivity of freshly cleaved single crystals of RbCl, RbBr and RbI and of an evaporated RbF film was measured at room temperature for photon energies between 10 and 30 eV using synchrotron radiation. With a resolution of 2 Å over the whole spectral range considerable new spectral features were observed in the region, where high energy valence band transitions occur and electrons from the first core level, the Rb $4p^+$ level, are excited. For all Rb halides excitation of the Rb $4p^+$ level starts at about 16 eV with an exciton multiplet which can be explained as being due to spin orbit splitting of the core level and to critical points at Γ and X in the conduction band. The energies of the multiplet are compared to transition energies of the 4p electrons in the free Rb^+ ion. The complex dielectric constant, the absorption coefficient and the energy loss function are derived from the reflectivity by means of a dispersion analysis. The results are compared with absorption and electron energy loss experiments on evaporated polycrystalline films.

[+] II. Institut für Experimentalphysik der Universität Hamburg, Hamburg, Germany

[‡] Sektion Physik der Universität München, München, Germany

Die Reflektivität von frisch gespaltenen RbCl-, RbBr- und RbJ-Einkristallen und einer RbF Aufdampfschicht wurden bei Zimmertemperatur mit Synchrotronstrahlung für Photonenenergien zwischen 10 und 30 eV gemessen. Bei einer Auflösung von 2 Å über den ganzen Spektralbereich konnten zahlreiche neue elektronische Anregungen vom Valenzband und dem ersten Rumpfniveau (Rb^+4p) gefunden werden. Die Übergänge vom Rb^+4p-Niveau beginnen für alle Rb-Halogenide bei etwa 16 eV mit einem Exzitonenmultiplett, das durch Spin-Bahn-Aufspaltung des Rumpfniveaus und kritische Punkte bei Γ und X im Leitungsband erklärt werden kann. Die Energien des Multipletts werden mit Anregungsenergien der 4p Elektronen des freien Rb^+ Ions verglichen. Aus der Reflektivität wurden mittels Dispersionsrelation die komplexe Dielektrizitätskonstante, der Absorptionskoeffizient und die Energieverlustfunktion berechnet. Die Ergebnisse werden mit Messungen der Absorption und des Energieverlustes von Elektronen an aufgedampften polykristallinen Schichten verglichen.

1. Introduction

During the last decade the low lying electronic transitions of the rubidium halides have extensively been studied for photon energies below 10 eV [1-4]. The spectra were interpreted in terms of excitons or interband transitions from the valence band which is formed by the outermost p-electrons of the halogen ion. Much effort has recently been spent on studying the optical properties of these materials by extending research into the extreme ultraviolet [5-11]. In this energy range electrons are excited from core states which represent initial states with well defined energy, since the electron bands are nearly flat. In comparison to the p-like valence band these states may have different symmetry (s or d) and the influence of selection rules can, therefore, be studied.

In the 10 to 30 eV range the optical properties of the Rb halides are partially determined by high energy transitions from the valence band. Excitation of the first core level (Rb^+4p) is expected at about 16 eV since at this energy the first electrons of the free Rb^+ ion are excited [12]. In the past, rubidium halides have been studied in this energy range by measuring the optical absorption [5,6] and electron energy loss [13] for thin evaporated films. The resolution in both kinds of experiments was limited to about 0.5 eV. Line source were used in the optical investigations and in the energy loss experiments the resolution was restricted by the energy width of the incident electron beam. Thin film absorption with improved resolution (3 Å) has only recently been reported for RbCl [7].

The aim of this work was threefold: 1. We wanted to investigate the Rb^+4p excitation of all Rb halides with higher resolution than was obtained before. We have, therefore, used the continuous spectrum of synchrotron radiation.

Knowledge of all details in the excitation spectra is necessary for a thorough understanding of the nature of electronic excitation. It has not been proved with certainty that the sharp lines found at the onset of core excitations are due more to excitons of the Frenkel or Wannier type or that these lines can simply be explained, as recently stated, by density of states effects [9,14]. 2. We wanted to determine the complex dielectric constant, particularly its imaginary part ε_2, which as yet was not available above 10 eV. All theoretical calculations are intended to yield this quantity. The shape and magnitude of ε_2 gives moredirect information about the physical nature of the excitation than a pure reflection, absorption or energy loss measurement. 3. Spectra of single crystals are expected to reveal best spectral fine structure as could be shown at lower energies [15]. We have, therefore, examined freshly cleaved single crystals, except for RbF, where we have studied thin film reflection.

2. Measurement of the Reflection Spectra

The reflection spectra of the Rb halides were measured at 15° angle of incidence from 10 to 30 eV at room temperature by means of a normal incidence monochromator [16] and a reflectometer [17] already described earlier. Using the synchrotron radiation of the Deutsches Elektronen-Synchrotron DESY as a light source [18,19] a resolution of 2 Å (i.e. 0.04 eV at 16 eV) was easily obtained over the whole energy range. We have examined single crystals, freshly cleaved before they were mounted into the sample holder, except for RbF which we have studied as thin film evaporated in situ from a tungsten boat onto a glass slide. The reflected light was detected by an open magnetic multiplier. The pressure before evaporation

and during the measurements was about 10^{-7} Torr. The light falling on the sample had a degree of polarization $(I_\perp - I_\parallel)(I_\perp + I_\parallel)^{-1}$ of about 0.98. The electric field vector of the main component ($I_\perp$) was lying perpendicular to the plane of incidence so that we could assume, with good accuracy, that for the subsequent dispersion analysis, the reflection measurements were performed for perpendicular polarized light.

In Fig. 1 the reflection spectra of the Rb halides are presented. The positions of the reflection maxima are listed in Table 1. In contrast to the relative spectral shape the absolute value of the reflectance was not determined with great accuracy since the reflected intensity and the incident intensity were not measured simultaneously. Therefore, in the case of RbCl, RbBr and RbI we preferred to normalize our measurements at 10 eV to those of Baldini and Bosacchi [4] who have made reflection measurements on the Rb halides up to this energy.

3. Dispersion Analysis

In order to obtain the complex dielectric constant $\hat{\varepsilon}(E) = \varepsilon_1(E) + i\varepsilon_2(E)$ [20] as a function of energy E a Kramers-Kronig transformation was applied to the reflectivity spectra R(E) of Fig. 1 [21]. The phase angle $\Theta(E_o)$ of the complex reflection coefficient $\hat{r}(E_o) = R(E_o)^{1/2}\, e^{i\Theta(E_o)}$ can be exactly determined for any energy E_o if the reflectivity R(E) is known over the entire energy range from zero to infinity by the integral transform

$$\Theta(E_o) = \frac{E_o}{\pi} P \int_0^\infty (E_o^2 - E^2)^{-1} \ln R(E)\, dE \qquad (1)$$

where P denotes the principal value.

The phase $\Theta(E_o)$ and the reflectivity $R(E_o)$ can be combined to calculate ε_2 and ε_1. Using Fresnel's equation for the reflection coefficient for perpendicular polarized light, which was used in this work and is denoted by the subscript s, the reflection coefficient for any angle of incidence ϕ is determined by

$$\hat{r}_s = R_s^{1/2}\, e^{i\Theta} = (a-ib-\cos\phi)(a-ib+\cos\phi)^{-1} \tag{2}$$

with $a^2-b^2 = \varepsilon_1-\sin^2\phi$ and $ab = \varepsilon_2/2$ (2a)

Equation (2) can be solved for a and b with given R_s, Θ and ϕ

$$\begin{aligned} a &= (1-R_s)\cos\phi\,(1+R_s-2R_s^{1/2}\cos\theta)^{-1} \\ b &= 2\cos\phi\,\sin\theta\,R_s^{1/2}(1+R_s-2R_s^{1/2}\cos\theta)^{-1} \end{aligned} \tag{3}$$

Using Eq. (2a) and Eq. (3) ε_1 and ε_2 can be calculated together with the complex index of refraction $\hat{n}=n+ik$ by Maxwell's relation $\hat{n}^2=\hat{\varepsilon}$. The formulas (1) - (3) have been used with $\phi = 15^o$ in order to determine ε_1, ε_2, the absorption coefficient $\mu = 2\,E_o k(\hbar c)^{-1}$ and the energy loss function $|\mathrm{Im}\hat{\varepsilon}^{-1}| = \varepsilon_2(\varepsilon_1^2+\varepsilon_2^2)^{-1}$ for comparison with previous measurements on the Rb halides.

The difficulties and errors in determinating the dielectric constant arise mainly from inaccurately measured absolute reflectivities and from uncertainties in the extrapolation of the integrand of Eq. (1). The energy range E_1 to E_2, for which the reflectivity has been studied, is limited by the experimental arrangement. In our case, this range was 10 to 30 eV. Below E_1 = 10 eV we have taken the data of Baldini and Bosacchi [4] and have extrapolated their values to lower energies by using the optical dielectric

constant ε_∞ [22] (Table 2) for calculating the reflectivity at zero energy. Such an extrapolation to low energies only includes the electronic component of the dielectric constant. At high energies, i.e. above E_2 = 30 eV, the reflectivity was extrapolated by

$$R(E) = cE^{-x} \tag{4}$$

where for x = 4 and $c = E_p^4/16$ we obtain the asymptotic behaviour of the normal incidence reflectivity of a free electron gas with plasma energy E_p neglecting damping. The numerical calculation was performed by an IBM 360/75 computer. The contribution of the reflectivity up to E_2 was computed by a polynom-integration-method (Simpson's rule). The contribution of the extrapolation (4) above E_2 was calculated in closed form:

$$\Theta_{E_2\to\infty} = \frac{1}{2\pi} \ln R(E_2) \ln \left|\frac{E_2-E_o}{E_2+E_o}\right| + \frac{x}{\pi} \sum_{\nu=1}^{\infty} \left(\frac{E_o}{E_2}\right)^{2\nu-1} (2\nu-1)^{-2} \tag{5}$$

During the calculation of $\Theta(E_o)$ x was adjusted so that no unphysical negative phases (or negative ε_2 values) occurred. The following x values were used: 6.8 for RbF, 7.0 for RbCl, 5.2 for RbBr and 6.6 for RbI.

Because of errors in the absolute reflectivity and the extrapolation the computed absolute values for ε_1 and ε_2 are not expected to be as accurate as values obtained by the multiangle reflection method, which, in the case of alkali halides, has only been used for the potassium halides in the same energy range [23]. An inaccurate normalization of the reflectivity by the same factor over the whole energy range does not affect the computed phase but changes the absolute values for ε_1 and ε_2 when Eq. (3) is used. The position and shape of the peaks, however, as well as their relative heights should be fairly correct.

4. Results and Comparison with Absorption and Energy Loss Measurements

Figures 2 - 5 show real and imaginary part of the dielectric constant computed from the reflection spectra of Fig. 1 by the procedure described in Sec. 3. The prominent multiplet structure which appears independent of the halogen component at about 16 eV in the reflection spectra as well as in the ε_2-spectra indicates the onset of transitions from the Rb^+4p core level. A detailed discussion of the multiplet is given in Sec. 5.

Figures 6 - 9 show the energy loss function $|\mathrm{Im}\hat{\varepsilon}^{-1}$ and the absorption coefficient μ as calculated from the values of Figs. 2 - 5. These values are compared with results on absorption [5-7] and electron energy loss [13] for thin evaporated films. In the latter experiments no absolute values for $|\mathrm{Im}\hat{\varepsilon}^{-1}|$ and μ could be determined; these values in Figs. 6-9 are, therefore, given in arbitrary units only. The sharp maxima in ε_2 and μ are shifted by 0.1 to 0.2 eV towards lower energy as compared to the position of the reflection maximum. The maxima of $\mathrm{Im}\hat{\varepsilon}^{-1}$, however, are shifted by a maximum of 1.0 eV to higher energy. The observed shifts are of the order of the half-width of the maxima. They were already expected from simple oscillator model calculations.

The measurements reported here apparently show a greater number of spectral details than previous work in this field. The reason for this is that Saito and coworkers have used line sources with one exception [7], whereas Creuzburg's data are obtained with a resolution of only about 0.5 eV, which was insufficient to resolve the multiplet fine structure. Therefore, the energy loss spectra only show broad and weak maxima. Apart from the fine structure which is observed in the reflection spectra using synchrotron radiation the positions of the main broad peaks, however, measured with different techniques, agree fairly well in most cases.

5. Discussion and Interpretation

RbF is the Rb halide with the largest energy gap. Its first excitation, the Γ_1 exciton, lies at 9.3 eV followed by the X_3 exciton at 10.9 eV (Fig. 1). Only a few further transitions from the valence band formed by halogen 2p electrons are observed below 15 eV. The valence band excitations of the Rb halides with heavier halogen ions, RbI for instance, show a greater variety. Its first exciton lies at much lower energy (5.5 eV) as compared to that of RbF. In Fig. 1 only the high energy part of the valence band transitions of RbI is presented. The greater complexity of the RbI spectrum is attributed to a broader valence band. The spin orbit splitting of the RbF valence band is only 0.05 eV, whereas for RbI it is as large as 1.2 eV [2]. A definite assignment of all the fine structure found between 10 and 16 eV has to wait for further theoretical investigations concerning exciton formation and density of states effects far beyond the threshold for valence band transitions.

The multiplet of sharp lines beginning at about 16 eV, which is approximately independent of the halogen ion, indicates the onset of transitions from the Rb^+4p core level. This level is the first below the valence band and is formed by the outermost 4p electrons of the alkali ion. The first transitions of the free Rb^+ ion are located at 15.68 eV ($4p^6 \rightarrow 4d$) and 16.72 eV ($4p^6 \rightarrow 5s$) [12]. Because of their small half-width (< 0.5 eV) the lines of the multiplet are attributed to excitonic transitions. The multiplet structure can be explained as caused by excitons coupled to the lower conduction band at Γ and X in the Brillouin zone, taking into account the large spin-orbit splitting of the Rb^+4p level. The spin-orbit splitting of the Rb^+4p level for the free ion is 0.92 eV [12]. One can expect at least four prominent core exciton lines, a quartet as sketched in Fig. 10. The energy difference between Γ_1 and X_3 in the conduction band has been calculated by A.B. Kunz et al. [24 - 26]. The

values obtained lie between 1.0 and 1.8 eV, cf. Table 2. For RbI the L_1 level was calculated to lie slightly below X_3 and is associated with a M_0-type singularity [25]. In this case one would expect the two high energy members of the quartet to be coupled to L_1 rather than to X_3.

The expected quartet (Fig. 10) is clearly observed for RbF (Fig. 1). Because of its magnitude the spin orbit splitting of the Rb^+4p level can easily be detected without cooling. For observation of the corresponding smaller splitting of the Na^+2p and K^+3p level in Na halides [27, 28] and K halides [23, 29] cooling is very useful. The individual interpretation of the exciton multiplet is given in the last column of Table 1. In the case of RbI only a triplet-structure is resolved. This fact can be explained by the almost equal energy differences associated with the spin-orbit splitting of the 4p-level and the distance Γ_1-X_3 in the conduction band. Two excitations form the middle line which thus becomes the strongest of the multiplet. From RbF to RbI the ratio of the intensity of the spin orbit partners of the Rb^+4p Γ-exciton, as derived from the ε_2-spectra after subtracting the background, decreases more and more starting with the value of about 2:1, which gives the ordinary degeneracy of the spin orbit components. The decreasing intensity ratio could be caused by increasing electron-hole exchange interaction [30].

If one assumes that Γ and X excitons have equal binding energies, one can compute the actual spin-orbit splitting (~0.9 eV) as well as the distance Γ_1-X_3 from the energy positions of the lines. The latter value is listed in Table 2 and compared to values from band calculations [24 - 26]. If, furthermore, the binding energy for the first valence band and core exciton

be the same, the energy distance between valence band and Rb^+4p level can be calculated, cf. Table 2.

In connection with the second strong core exciton $\Gamma(1/2)$ at about 17.1 eV a weak maximum or shoulder respectively is observed at its low energy side for RbCl, RbBr and RbI. One could interprete this feature as the second member of a Wannier series or the onset of interband absorption from the Rb^+4p level. With this interpretation an exciton binding energy of about 0.5 eV is estimated.

A different interpretation for the weak maximum can be given in terms of localized transitions associated with the free Rb^+ ion. In this picture the weak maximum may be attributed to a weak atomic-like transition from the Rb^+4p level to the 4d $[1/2]^o$, J=1 state which, for the free ion, is found at 15.68 eV [12] and is shifted to 16.7 eV in the solid state (j-l coupling notation of ref. 12 is used for classifying the excited states). A similar correspondence has recently been suggested in the case of RbCl [7]. If we consistently follow the picture of localized free ion transitions modified by the crystal field we can reinterprete the strong lines of the quartet denoted by Γ and X in Fig. 1 as follows: According to ref. 12 the first line may be associated to the free ion state 5s $[3/2]^o$, J=1 at 16.72 eV, the second line to 5s' $[1/2]^o$, J=1 at 17.78 eV, the third line to 4d $[3/2]^o$, J=1 at 17.43 eV and the fourth line to 4d' $[3/2]^o$, J=1 at 18.05 eV [12]. Together with the already discussed weak 4d $[1/2]^o$, J=1 transition at 15.7 eV a qunitet correspondence between the solid and the free ion is established (cf. Table 1). In order to understand the energy shifts observed in the solid one has to assume that by the crystal field the s-transitions are shifted to smaller energies by about 0.5 eV and the d-transitions to higher energies by about 1 eV. A similar quintet structure with similar energy shifts could recently be observed for the Cs halides at

the onset of transitions from the Cs^+5p level [3]. The excitations at energies above 18 eV are due to transitions to higher conduction bands or are associated with higher free ion levels respectively. As yet, no detailed interpretation can be given for these transitions. The decrease of the reflectivity beyond about 27 eV may be correlated with the ionization limit of the free Rb^+ ion which is found at 27.5 eV and 28.4 eV respectively [12].

Deeper lying core states of the RbCl have recently been studied, i.e. the Cl^-2p and Rb^+3d level [9]. In analyzing their data the authors stated that all observed structure can be understood in terms of interband transitions (i.e. density of states) taking into account spin-orbit splitting. They claimed that no excitons are necessary to understand the spectral features. The width of the observed maxima of these core excitations is relatively large (of the order of 1 eV), whereas the lines associated with the Rb^+4p level are less than 0.5 eV wide. Such sharp structures can probably not be explained simply by density of states effects. If both statements are correct one apparently has to assume that core excitons exist; for deeper core states, however, the probability for exciton formation decreases.

Acknowledgment

We would like to thank R. Klucker and E.E. Koch for help during the measurements and R. Haensel and W. Steinmann for discussions. We are grateful to the staff of the synchrotron radiation group at DESY for technical assistance.

References

1. J.E. Eby, K.J. Teegarden, and D.B. Dutton, Phys.Rev. 116, 1099 (1959)
2. K. Teegarden and G. Baldini, Phys.Rev. 115, 896 (1967)
3. D.M. Roessler and W.C. Walker, J.Opt.Soc.Am. 57, 677 (1967)
4. G. Baldini and B. Bosacchi, Phys.Rev. 166, 863 (1968)
5. H. Saito, S. Saito, R. Onaka and B. Ikeo, J.Phys.Soc. Japan 24, 1096 (1968)
6. H. Saito, S. Saito and R. Onaka, J.Phys.Soc. Japan 28, 699 (1970)
7. H. Saito, M. Watanabe, A. Ejiri, S. Saito, H. Yamashita, T. Shibaguchi, H. Nishida and S. Yamaguchi, Solid State Comm. 8, 1861 (1970)
8. M. Cardona, R. Haensel, D.W. Lynch and B. Sonntag, Phys.Rev. B 2, 1117 (1970)
9. F.C. Brown, C. Gähwiller, H. Fujita, A.B. Kunz, W. Scheifley, and N. Carrera, Phys.Rev. B 2, 2126 (1970)
10. A.S. Vinogradov, T.M. Zimkina, and Yu.F. Mal'tsev, Soviet Physics Solid State 11, 2721 (1970), translated from Fisika Tverdogo Tela 11, 3354 (1969)
11. Y. Iguchi, Science of Light (Tokyo) 19, 1 (1970)
12. C.E. Moore, Atomic Energy Levels, Nat.Bur.Std. (U.S.), Circ. No. 467, Vol. II (1958)
13. M. Creuzburg, Z. Physik 196, 433 (1966)
14. N.O. Lipari and A.B. Kunz, Phys.Rev. B 3, 491 (1971)
15. G. Baldini, A. Bosacchi, and B. Bosacchi, Phys.Rev. Letters 23, 846 (1969)
16. M. Skibowski and W. Steinmann, J.Opt.Soc.Am. 37, 162 (1967)
17. B. Feuerbacher, M. Skibowski and R.P. Godwin, Rev.Sci.Instr. 40, 305 (1969)

18. R. Haensel and C. Kunz, Z. Angew. Physik 23, 276 (1967)

19. R.P. Godwin, Springer Tracts in Modern Physics 51, 1 (1969)

20. Complex quantities are denoted by ^.

21. The procedure was similar to that described by D.M. Roessler (Brit.J.Appl.Phys. 16, 1359 (1965))
and M. Cardona in Optical Properties of Solids, Plenum Press 1969, Chap. 6.

22. Landolt-Börnstein, Zahlenwerte und Funktionen aus Physik, Chemie, Astronomie, Geophysik und Technik Vol. II/6, p. 461 (1959), Vol. II/8, p. 2-410 (1962), Springer Verlag

23. D. Blechschmidt, R. Klucker and M. Skibowski, phys.stat.sol. 36, 625 (1969)

24. A.B. Kunz, phys.stat.sol. 29, 115 (1968)

25. A.B. Kunz, J.Phys.Chem. Solids 31, 265 (1970)

26. A.B. Kunz, T. Miyakawa, and W.B. Fowler (to be published)

27. R. Haensel, C. Kunz, T. Sasaki and B. Sonntag, Phys.Rev. Letters 20, 1436 (1968)

28. S. Nakai, T. Ishii and T. Sagawa, J.Phys.Soc. Japan 30, 428 (1971)

29. D. Blechschmidt, R. Haensel, E.E. Koch, U. Nielsen and M. Skibowski, phys.stat.sol. 44, (1971), and references given in this work

30. Y. Onodera and Y. Toyozawa, J.Phys.Soc. Japan 22, 833 (1967)

31. D. Blechschmidt, V. Saile, M. Skibowski and W. Steinmann to be published

RbF	RbCl	RbBr	RbI		
9.3					
∿10.2s					
10.9	9.0				
12.8	10.0	10.8			
	12.3	11.4	10.0		
∿15.4s	∿13.7s	∿12.2s	∿10.9s	valence band excitation	
		∿15.3s	∿11.6s		
			13.1		
			13.9		
			14.9		
			15.6		
16.1	16.1	16.2	16.2	$4p(3/2)\rightarrow\Gamma_1$	$5s\ [3/2]^o$
16.8	16.7	16.7	16.7		$4d\ [1/2]^o$
17.0	17.1	17.0	17.2	$4p(1/2)\rightarrow\Gamma_1$	$5s'\ [1/2]^o$
17.8	17.5	17.4		$4p(3/2)\rightarrow X_3$	$4d\ [3/2]^o$
18.7	18.3	18.3	18.1	$4p(1/2)\rightarrow X_3$	$4d'\ [3/2]^o$
∿20.6s	∿18.6s		19.1		
22.0	21.8	21.2	20.7		
26.5	24.6	23.8	23.1		

Table 1: Position of the reflection maxima (in eV, accuracy ±0.05 eV for the sharp peaks). Tentative correlation with the low lying J=0→1 transitions of the free Rb^+ ion (last column)

	Γ_1-X_3		E_{VB}	E_{Rb}	$E_{Rb}-E_{VB}$	ε_∞
RbF	1.7 eV	(1)	9.3 eV	16.1 eV	6.8 eV	1.93
	1.7	(2)				
RbCl	1.35	(1)	7.4 [4]	16.1	8.7	2.19
	1.4	(2)				
RbBr	1.13	(1)	6.4 [4]	16.2	9.8	2.33
	1.2	(2)				
RbI	0.9	(1)	5.5 [4]	16.2	10.7	2.63
	1.0	(2)				

Table 2:

Energy distance Γ_1-X_3 as calculated by A.B. Kunz et al. [24-26] (1) and the value (2) obtained by subtracting the energy of the $\Gamma(3/2)$ Rb^+4p-exciton from that of the $X(3/2)$ Rb^+4p-exciton. E_{VB}, the position of the $\Gamma(3/2)$ valence band exciton, E_{Rb} the position of the $\Gamma(3/2)$ Rb^+4p-exciton. $E_{Rb}-E_{VB}$ represents the band distance between the top of the valence band and the Rb^+4p (3/2) level. ε_∞ is the optical dielectric constant [22].

Figure Captions

Fig. 1 Reflectivity spectra of RbCl, RbBr and RbI single crystals and of an evaporated RbF film.

Fig. 2 Dielectric constants ε_1 and ε_2 of RbF

Fig. 3 Dielectric constants ε_1 and ε_2 of RbCl

Fig. 4 Dielectric constants ε_1 and ε_2 of RbBr

Fig. 5 Dielectric constants ε_1 and ε_2 of RbI

Fig. 6 Energy loss function and absorption coefficient of RbF (absolute scale, solid line) compared with the relative values obtained by Creuzburg [13] and Saito et al. [5, 6] respectively

Fig. 7 Energy loss function and absorption coefficient of RbCl (absolute scale, solid line) compared with the relative values obtained by Creuzburg [13] and Saito et al. [7] respectively

Fig. 8 Energy loss function and absorption coefficient of RbBr (absolute scale, solid line) compared with the relative values obtained by Creuzburg [13] and Saito et al. [5, 6] respectively

Fig. 9 Energy loss function and absorption coefficient of RbI (absolute scale, solid line) compared with the relative values obtained by Creuzburg [13] and Saito et al. [5, 6] respectively

Fig. 10 The conduction and valence band for RbF as calculated by A.B. Kunz et al. [26]. The Rb^+4p core level is added from experimental data.

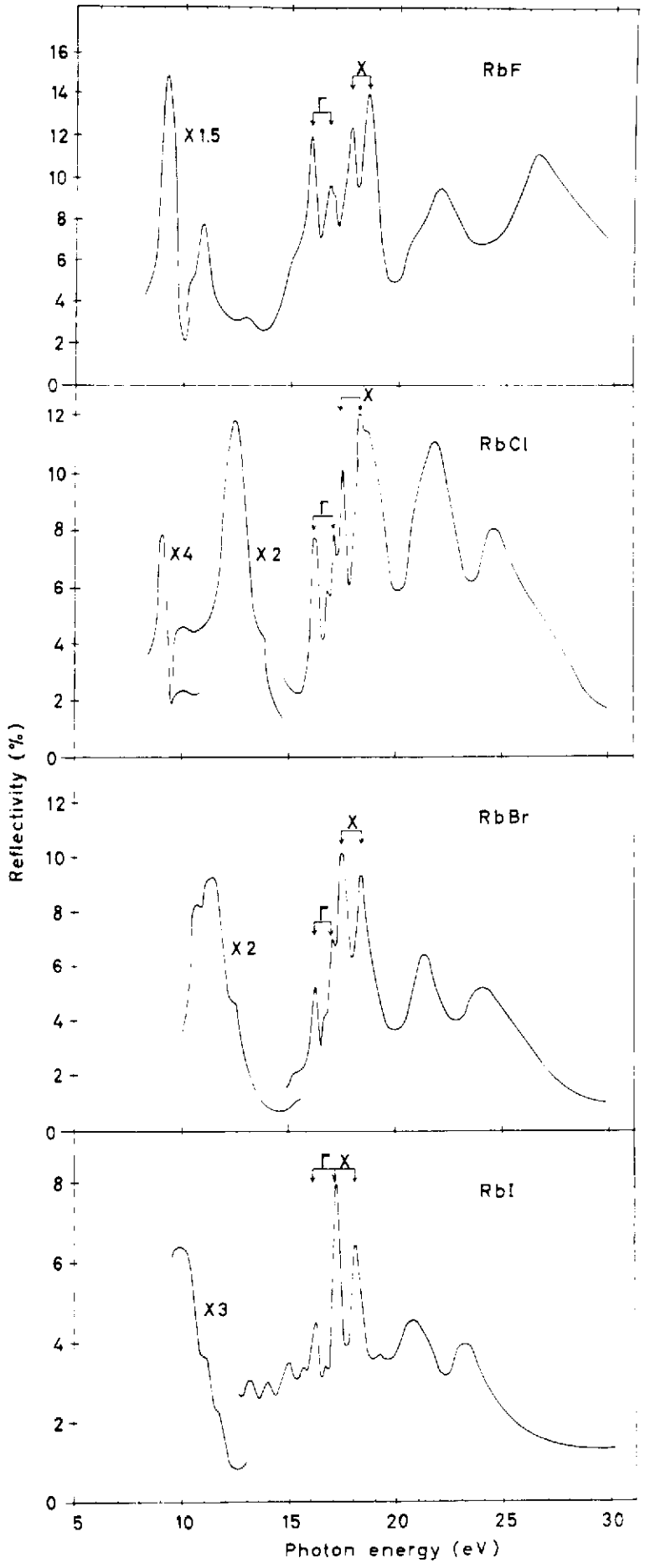
RbF
X 1.5
Γ
X
RbCl
X4
X 2
RbBr
X 2
RbI
X3
Reflectivity (%)
Photon energy (eV)
0
2
4
6
8
10
12
14
16
5
10
15
20
25
30

Fig. 1

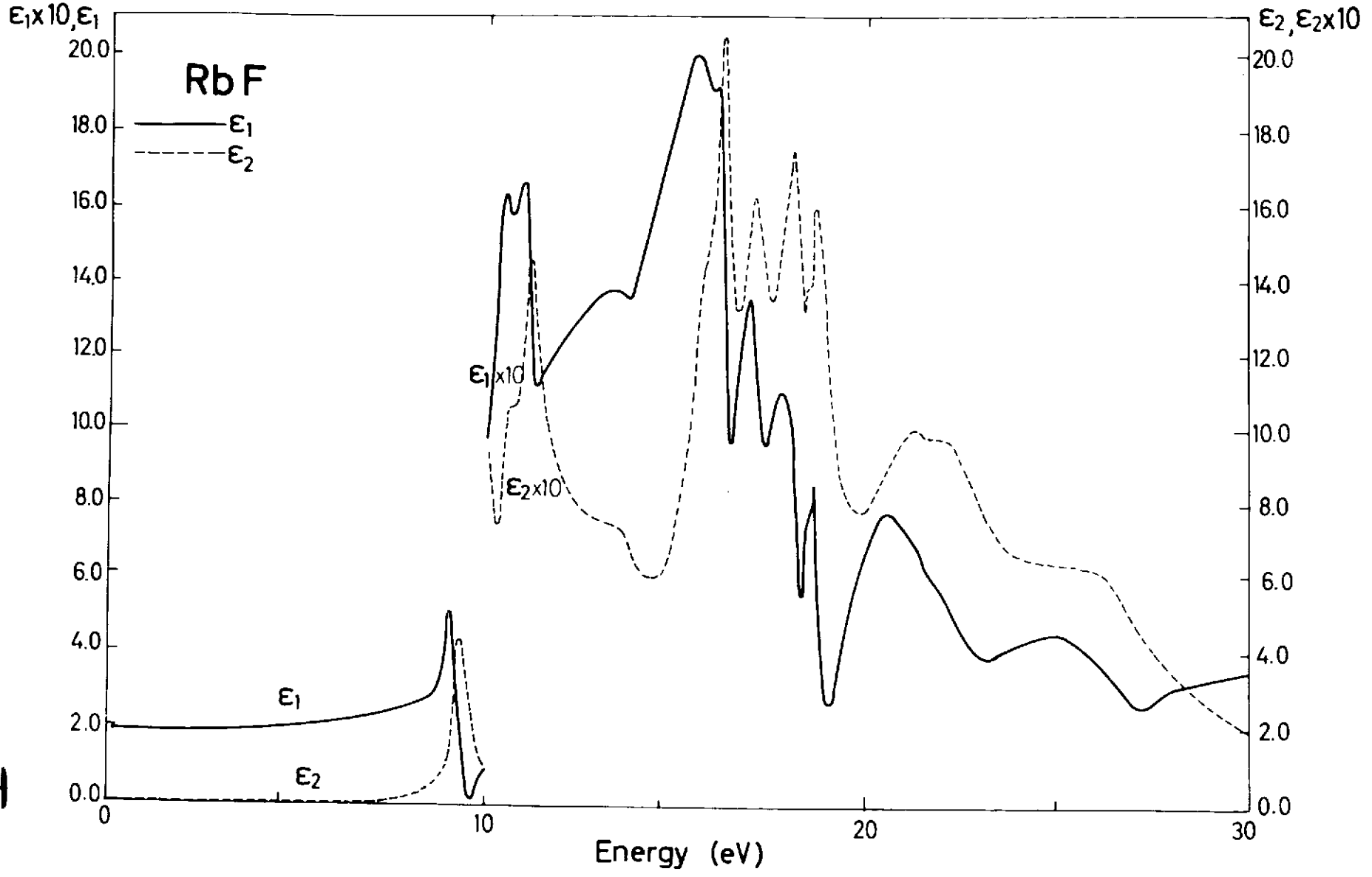
ε1x10, ε1
ε2, ε2x10
RbF
ε1
ε2
ε1x10
ε2x10
ε1
ε2
Energy (eV)
0
10
20
30
0.0
2.0
4.0
6.0
8.0
10.0
12.0
14.0
16.0
18.0
20.0

Fig. 2

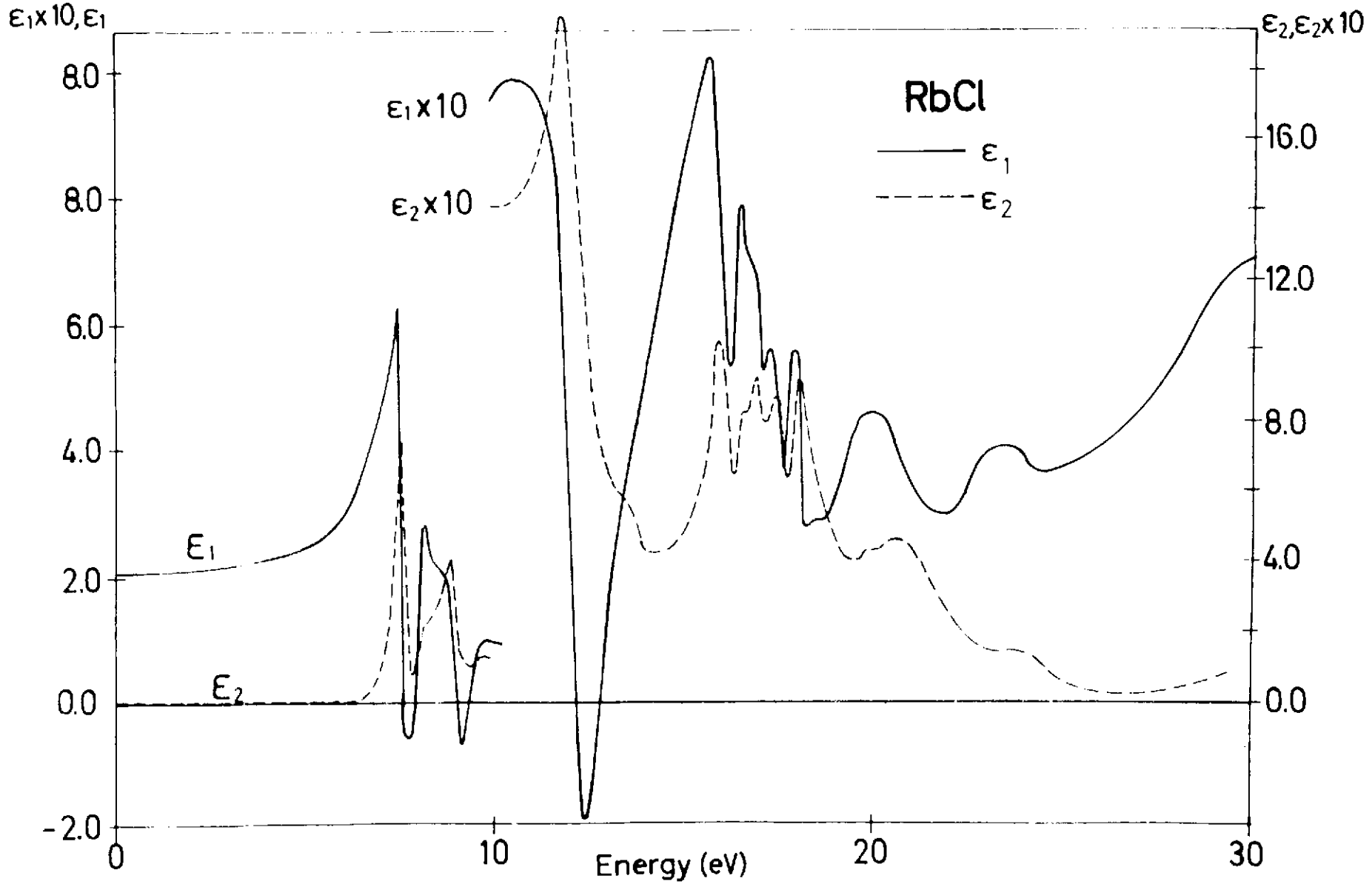
ε₁x10, ε₁
ε₂, ε₂x10
RbCl
ε₁
ε₂
ε₁x10
ε₂x10
E₁
E₂
8.0
8.0
6.0
4.0
2.0
0.0
-2.0
16.0
12.0
8.0
4.0
0.0
0
10
20
30
Energy (eV)

شكل ٣

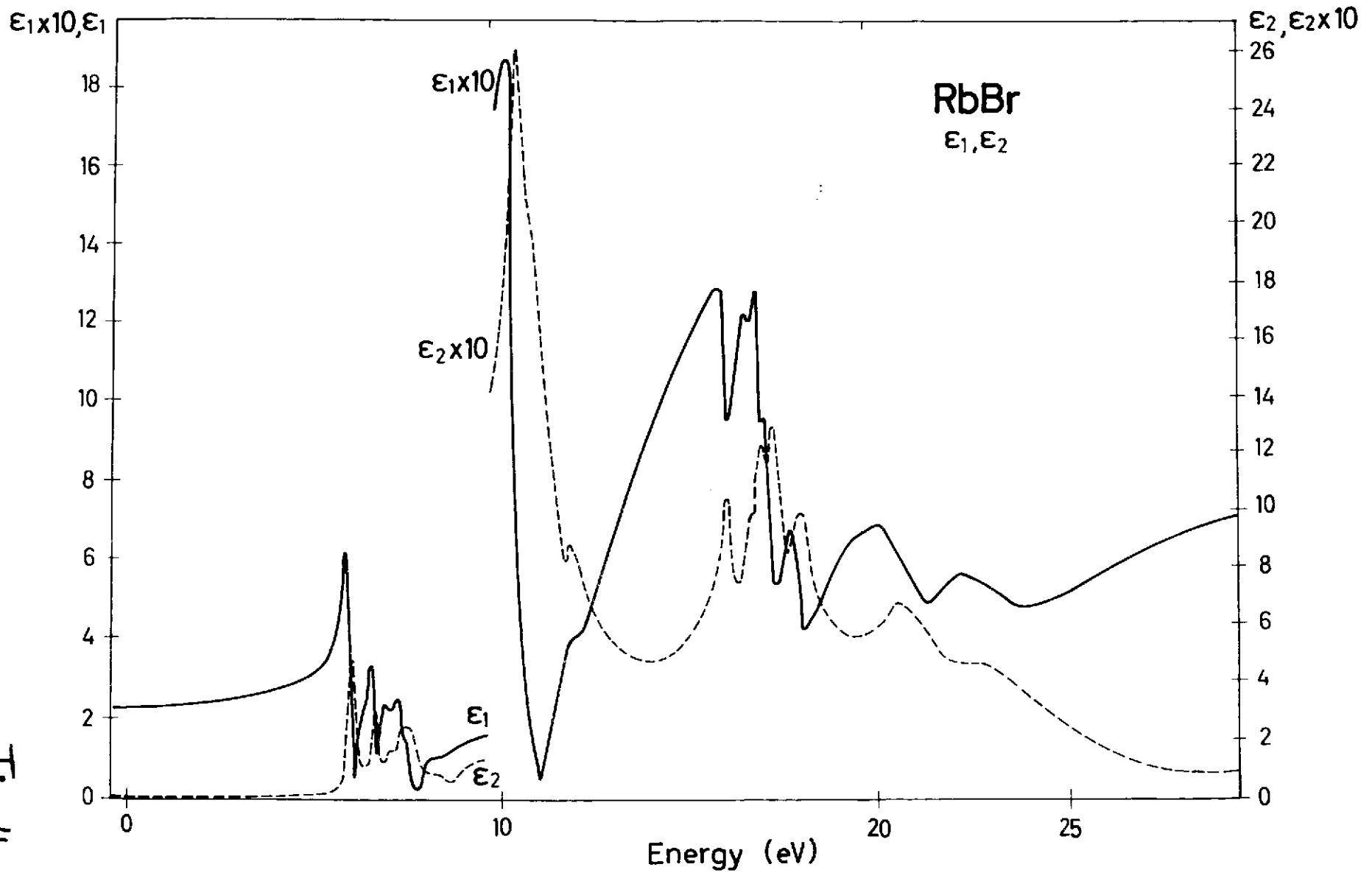
ε1x10,ε1
ε2,ε2x10
ε1x10
ε2x10
RbBr
ε1,ε2
ε1
ε2
Energy (eV)
0
10
20
25
0
2
4
6
8
10
12
14
16
18
0
2
4
6
8
10
12
14
16
18
20
22
24
26

Fig. 4

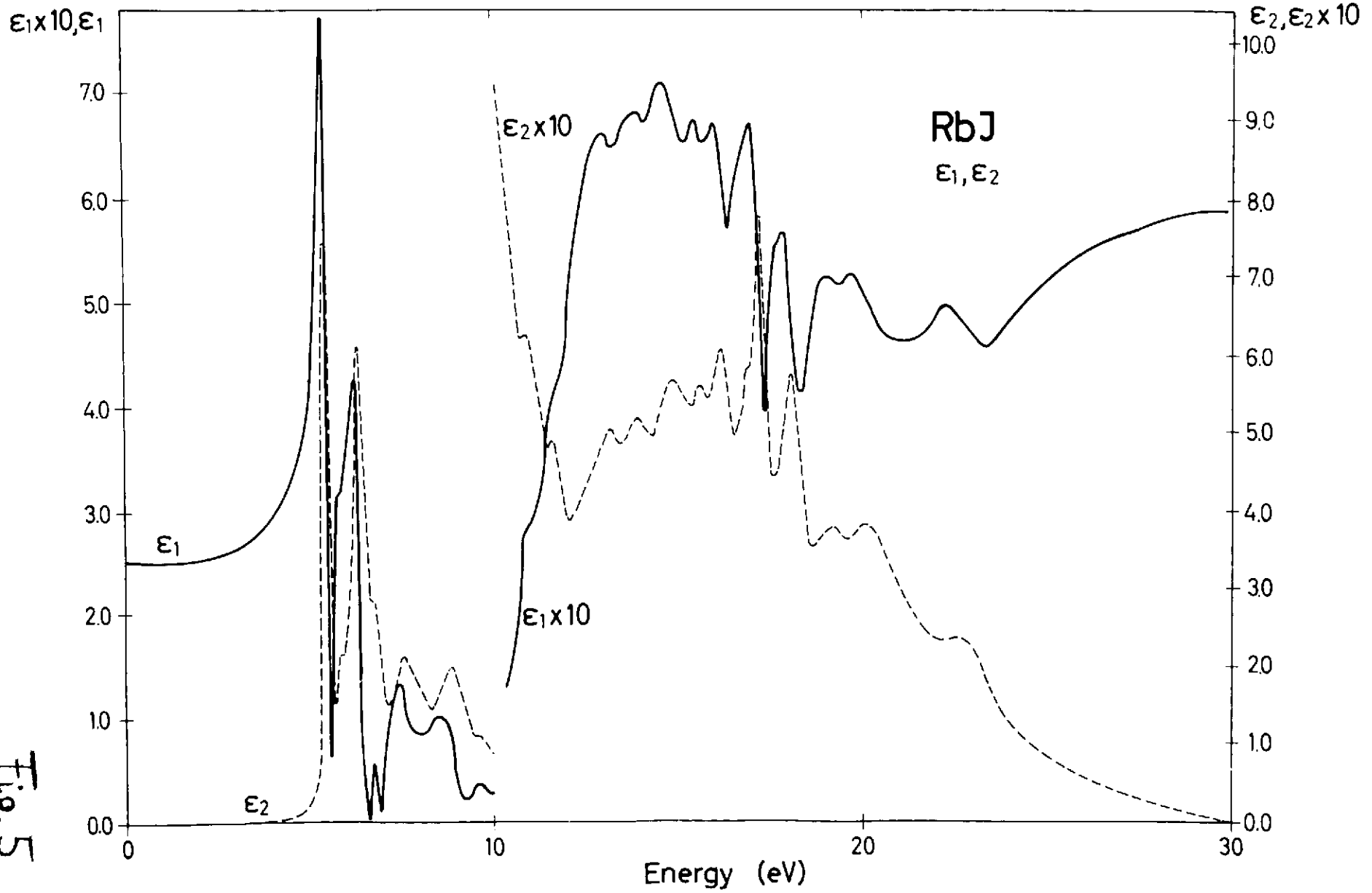
ε1x10,ε1
ε2,ε2x10
RbJ
ε1, ε2
ε2x10
ε1
ε2
ε1x10
Energy (eV)
0
10
20
30
0.0
1.0
2.0
3.0
4.0
5.0
6.0
7.0
8.0
9.0
10.0

Fig. 5

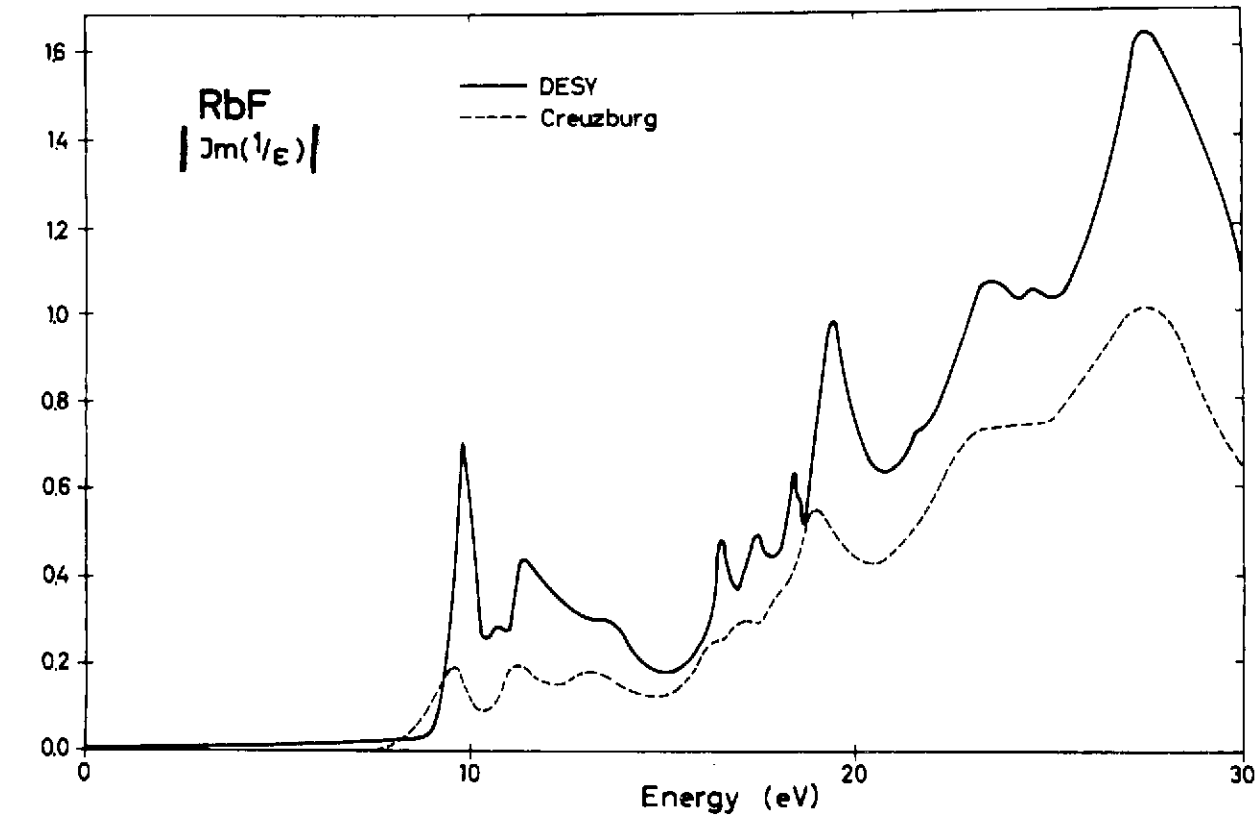
RbF
Im(1/ε)
DESY
Creuzburg
1.6
1.4
1.2
1.0
0.8
0.6
0.4
0.2
0.0
0
10
20
30
Energy (eV)

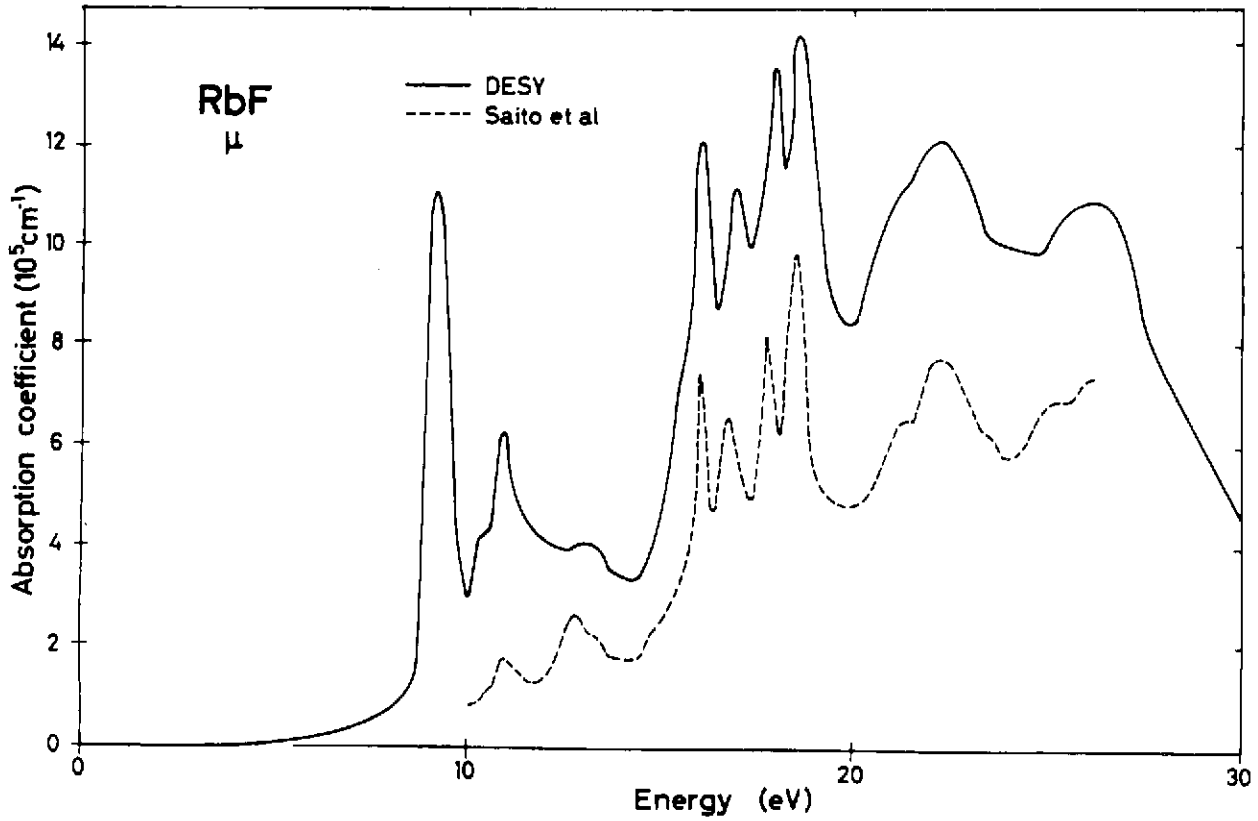
RbF
μ
DESY
Saito et al
Absorption coefficient (10⁵cm⁻¹)
14
12
10
8
6
4
2
0
0
10
20
30
Energy (eV)

Fig. 6

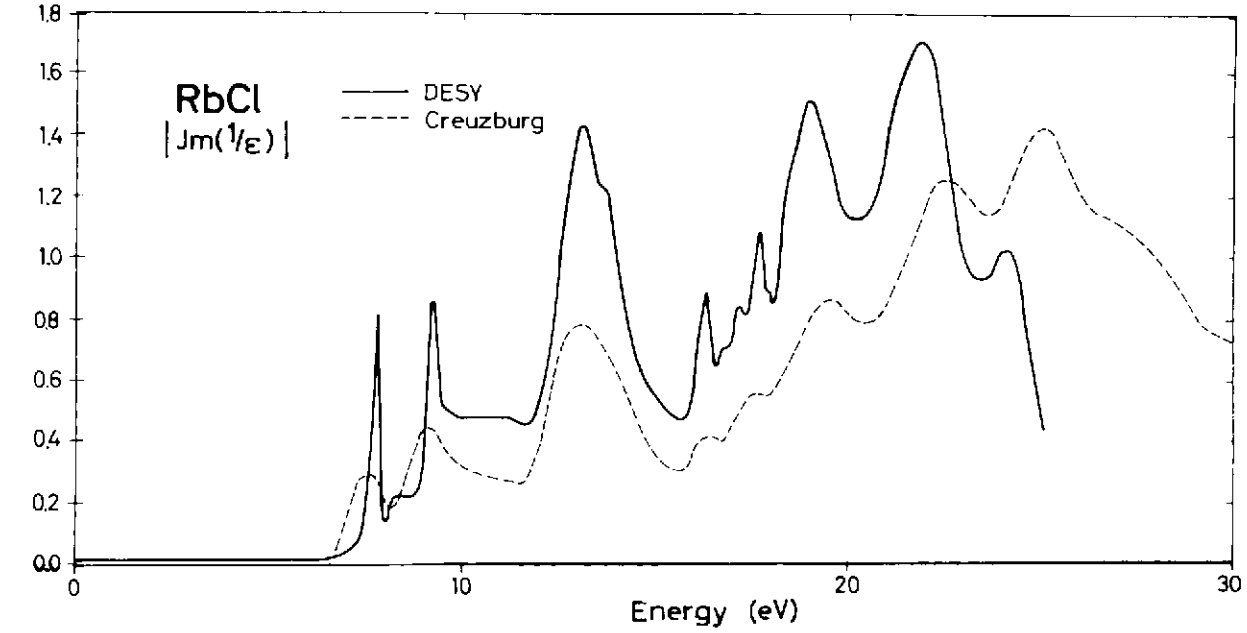
RbCl
| Im(1/ε) |
DESY
Creuzburg
1.8
1.6
1.4
1.2
1.0
0.8
0.6
0.4
0.2
0.0
0
10
20
30
Energy (eV)

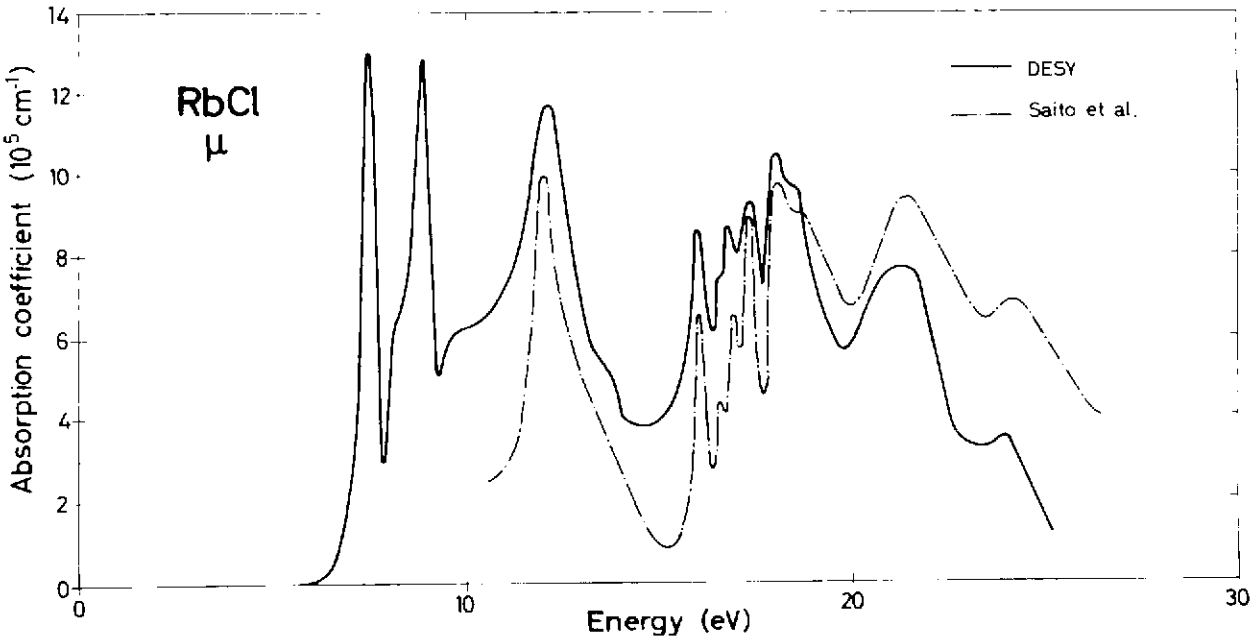
RbCl
μ
DESY
Saito et al.
Absorption coefficient (10^5 cm^-1)
14
12
10
8
6
4
2
0
0
10
20
30
Energy (eV)

Fig. 7

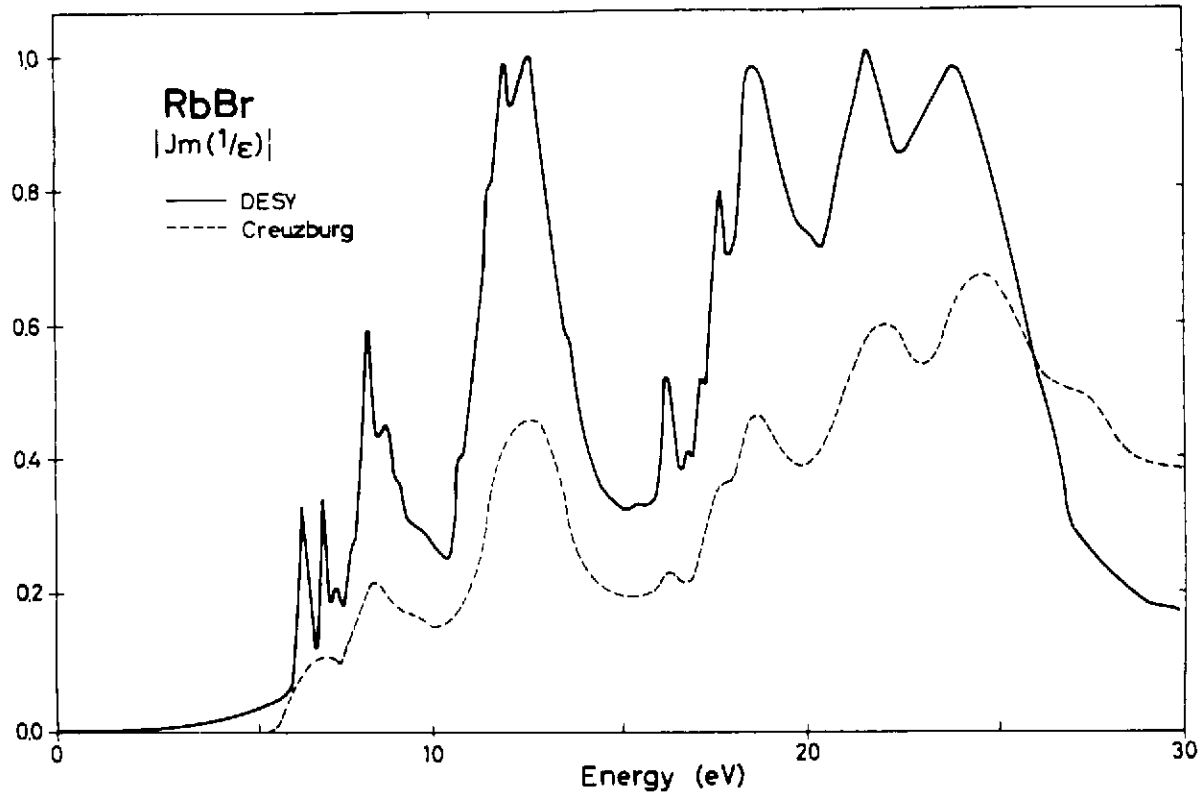
RbBr
|Jm(1/ε)|
DESY
Creuzburg
1.0
0.8
0.6
0.4
0.2
0.0
0
10
20
30
Energy (eV)

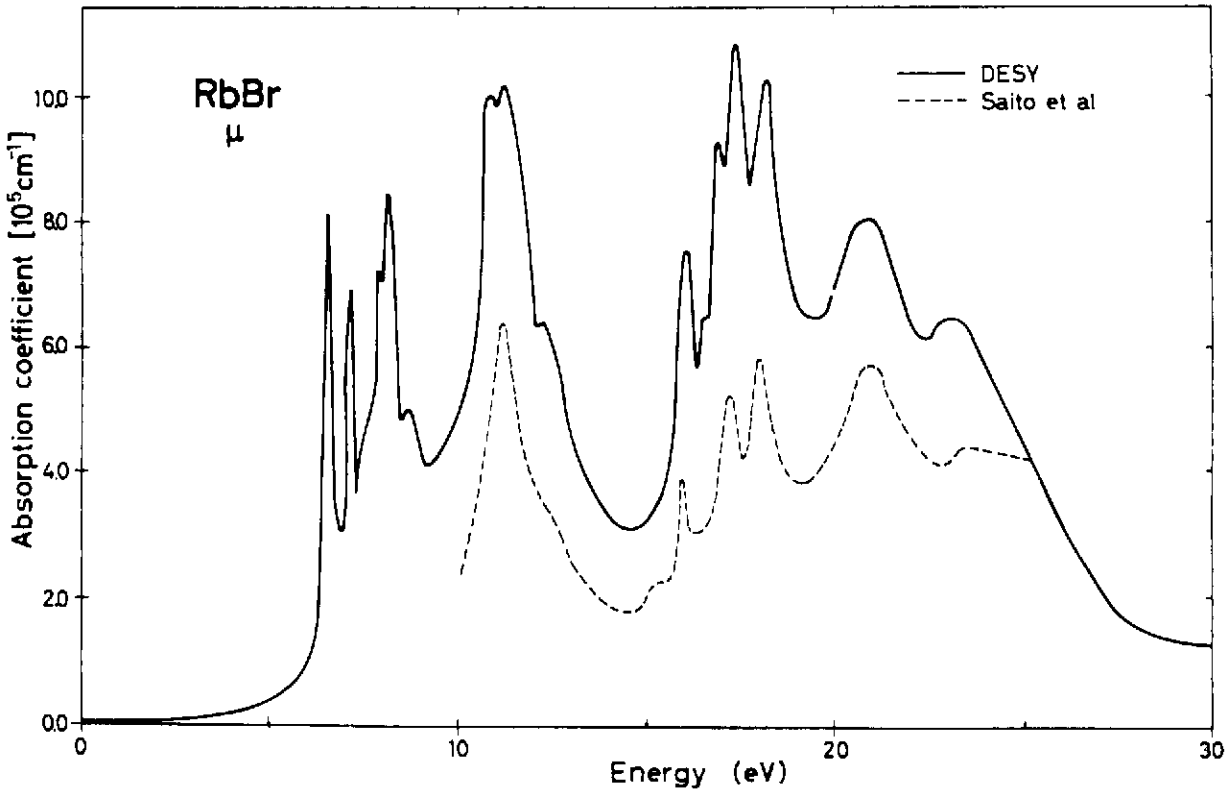
RbBr
μ
DESY
Saito et al
Absorption coefficient [10⁵cm⁻¹]
10.0
8.0
6.0
4.0
2.0
0.0
0
10
20
30
Energy (eV)

Fig. 8

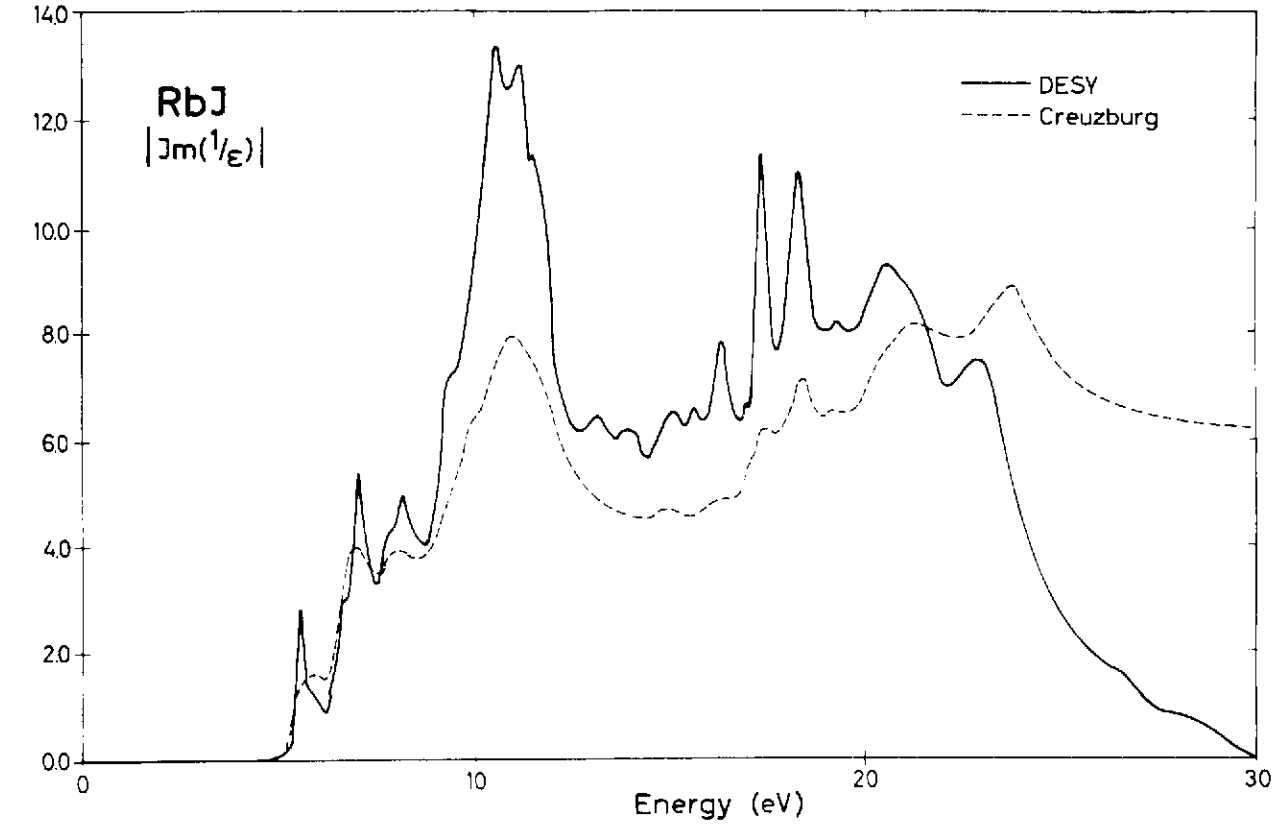
RbJ
$|Im(1/\varepsilon)|$
DESY
Creuzburg
14.0
12.0
10.0
8.0
6.0
4.0
2.0
0.0
0
10
20
30
Energy (eV)

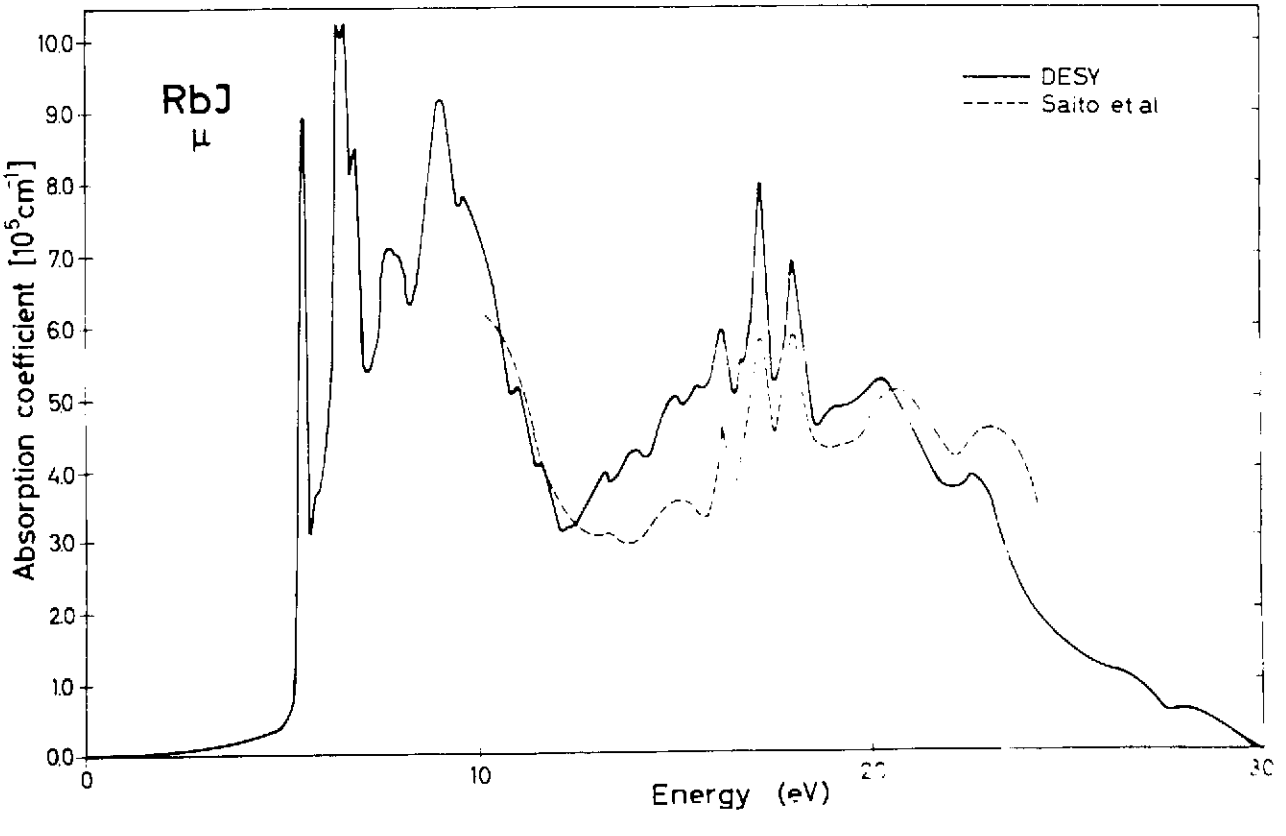
RbJ
μ
DESY
Saito et al
Absorption coefficient [$10^5 cm^{-1}$]
10.0
9.0
8.0
7.0
6.0
5.0
4.0
3.0
2.0
1.0
0.0
0
10
Energy (eV)

Fig. 9

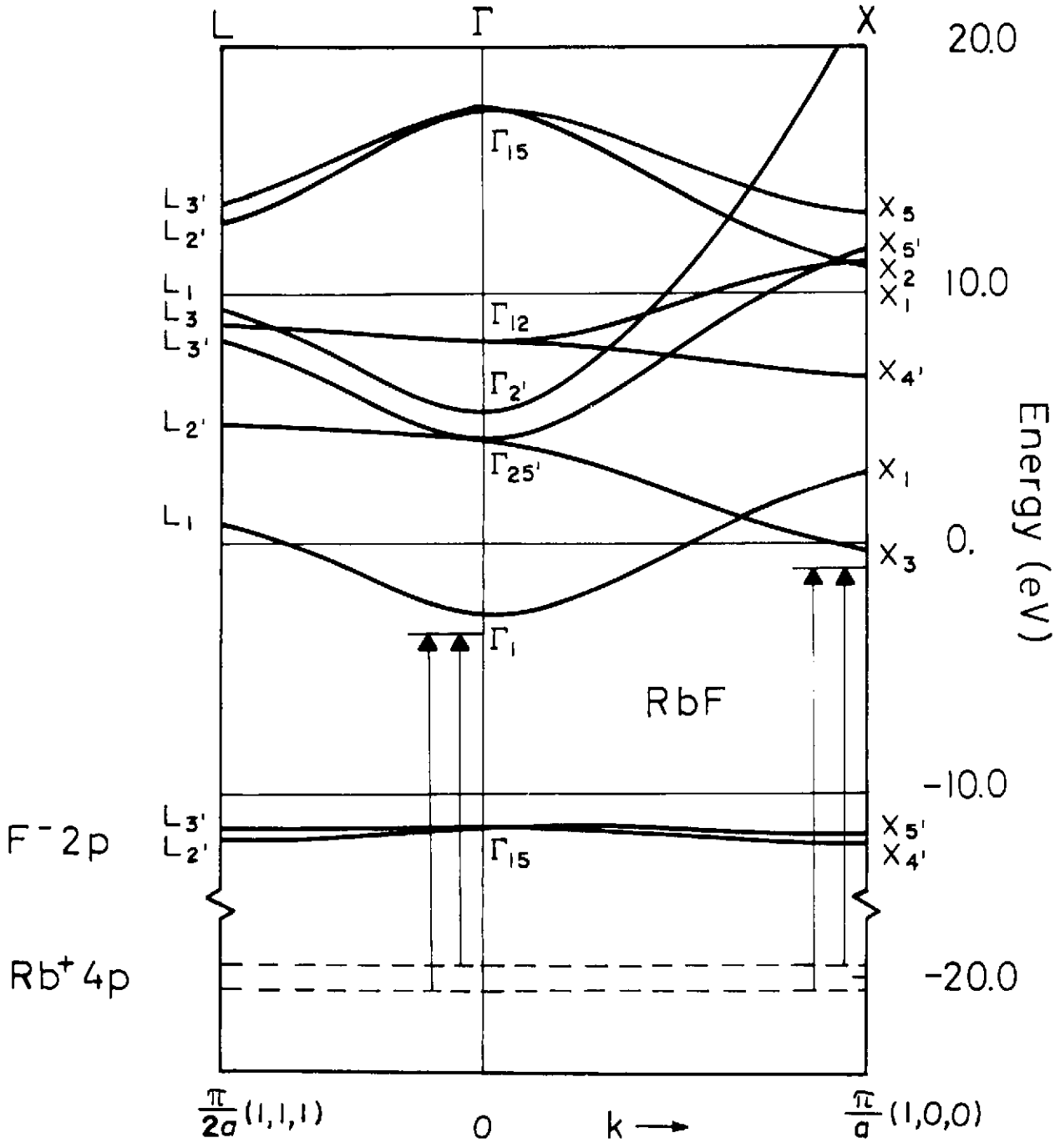
L
Γ
X
20.0
10.0
0.
-10.0
-20.0
Energy (eV)
Γ15
Γ12
Γ2'
Γ25'
Γ1
L3'
L2'
L1
L3
L3'
L2'
L1
X5
X5'
X2
X1
X4'
X1
X3
RbF
L3'
L2'
Γ15
X5'
X4'
F⁻ 2p
Rb⁺ 4p
π/2a (1,1,1)
0
k →
π/a (1,0,0)

Fig. 10